Improved Nyquist Pulses Produced By A Filter with Senary Piece-wise Polynomial Frequency Characteristic

Alexandra Ligia BALAN[1], Nicolae Dumitru ALEXANDRU[2]
[1]*Stefan cel Mare University of Suceava, 720229, Romania*
[2]*Gh. Asachi Technical University of Iaşi, 700506, Romania*
alexandra@eed.usv.ro

[1]***Abstract*—A novel family of inter-symbol interference (ISI) free pulses generated by improved Nyquist filters with a frequency characteristic composed of six parabolic pieces is proposed. We studied the performance of the new pulses in terms of the ISI error probability when the impulse response is sampled with a timing offset. To illustrate the achieved improvement, the new pulses are compared with other performing pulses that were reported in the literature. Simulation results show that comparable or enhanced ISI performance can be obtained at reasonable complexity.**

***Index Terms*—inter-symbol interference, Nyquist filter, error probability, filter design.**

I. INTRODUCTION

Our article introduces and investigates a novel family of pulses, which are generated by a Nyquist filter.

In several recent works [3-9], the improved Nyquist filters (INFs) have received a great deal of attention and have been successfully used in order to achieve improved performance in terms of error probability and maximum distortion when the impulse response is sampled off-center due to a timing error using as a basis of comparison the raised cosine (RC) pulse. L. E. Franks [1] and F. S. Hill Jr. [2] are credited with the first contributions on this theme.

As stated by Nyquist's first criterion, in order to obtain ISI-free transmission the pulse shape should have zero crossings at the sampling moments, with the exception of current one. Also, the pulse tails should decay fast. Several new ISI-free pulses [3-9] were reported and analyzed. They asymptotically decay as t^{-3} and as t^{-2}, respectively. In [8] were used pulse shapes which provide Asymptotic Decay Rates (ADR) of t^{-k}, for integer values of k ranging between 2 and 4.

So far, we found that the use of a of frequency characteristic having a concave shape in the transition region close to $B(1-\alpha)$, and a convex one close to $B(1+\alpha)$, in view of the odd-symmetry, will determine an INF that exhibits pulse tails having a smaller slope in the vicinity of ideal sampling moments. This behavior is due to a transfer of energy into the high spectral region [9], [12], [13].

Details of the proposed filter characteristic design and results are presented and discussed in the following sections.

This work was supported by the project CNCSIS-UEFISCDI Project number RU-107/2010.

Digital Object Identifier 10.4316/AECE.2014.02021

II. FILTER DESIGN AND IMPULSE RESPONSE

In [10] we proposed and investigated a novel approach for obtaining a family of Nyquist pulses with an ADR of t^{-2} with improved performance in terms of ISI, as compared with recent pulses. The pulses were generated by an INF with a piece-wise frequency characteristic consisting of four pieces using concave and convex parabolic segments.

The generated pulse is optimized by varying the coordinates of the delimiting points of the pieces in order to decrease the value of the error probability to a minimum, assuming that the impulse response is sampled off-center.

The equation of a parabolic function $H_i(f)$ with the vertex at the point (x_0, y_0) passing through (x_1, y_1) is

$$H(f) = \frac{y_1 - y_0}{(x_1 - x_0)^2}(f - x_0)^2 + y_0 \qquad (1)$$

The parabola has a concave shape if $x_0 > x_1$, and $y_0 < y_1$. The condition $x_0 < x_1$, and $y_0 > y_1$ determines a convex-shaped parabola having the vertex at (x_1, y_1) and passing through (x_0, y_0).

We extend the approach in [10] considering an INF with a frequency characteristic consisting of six pieces, each piece being either a convex or a concave parabolic segment. There is a set of six convex parabolic pieces denoted as $A_i, i = 1,2,\cdots 6$ and six concave ones denoted as $A_i', i = 1,2,\cdots 6$.

Choosing a convex piece from the set $A_i, i = 1,2, \textit{and } 3$ in the frequency range below Nyquist frequency B, its counterpart above B will be a concave one from the set $A_i', i = 4,5, \textit{and } 6$. Also, the reciprocal is valid.

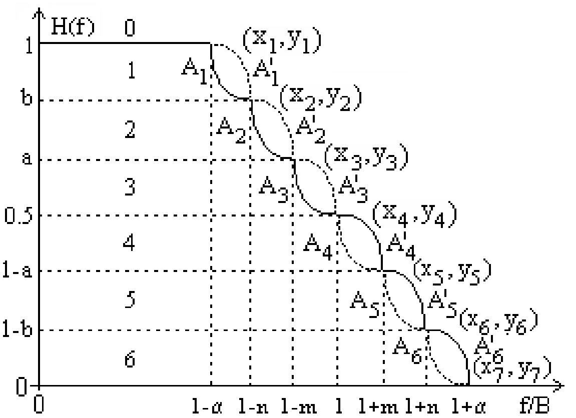

Figure 1. Frequency characteristics of proposed filters

TABLE I. COORDINATES OF DELIMITING POINTS OF THE PROPOSED INF FILTER 1

Piece No. i	Frequency Characteristic	x_{0i}	x_{1i}	y_{0i}	y_{1i}
1	$H_1(f)$	B(1-n)	B(1-α)	b	1
2	$H_2(f)$	B(1-m)	B(1-n)	a	b
3	$H_3(f)$	B(1-m)	B	a	0.5
4	$H_4(f)$	B	B(1+m)	0.5	1-a
5	$H_5(f)$	B(1+m)	B(1+n)	1-a	1-b
6	$H_6(f)$	B(1+n)	B(1+α)	1-b	0

In view of the odd-symmetry, there will be a convex-concave relationship given by

$$A_{3-i} \leftrightarrow A'_{4+i}\,,\; i = 0,1,\; and\; 2 \tag{2}$$

One can form a set $\boldsymbol{F}$ of 8 filters with piece-wise parabolic frequency characteristic denoted as

$$\begin{gathered} F = \{A_1A_2A_3A_4'A_5'A_6',\; A_1'A_2A_3A_4'A_5'A_6, \\ A_1A_2'A_3A_4'A_5A_6',\; A_1A_2A_3'A_4A_5'A_6', \\ A_1'A_2'A_3A_4'A_5A_6,\; A_1'A_2A_3'A_4A_5'A_6, \\ A_1A_2'A_3'A_4A_5A_6',\; A_1'A_2'A_3'A_4A_5A_6\} \end{gathered} \tag{3}$$

For convenience we will denote the filters using the first 3 parabolic pieces. So, we denote concave by *K* and convex by *C*. For example, the filter defined by $A_1A_2A_3'A_4'A_5'A_6$ will be denoted as *KKC*.

The frequency characteristics of the proposed filters can be inferred from Fig.1 in conjunction with Eq. (3).

Table I reports the coordinates of the end-points which define the six component parabolic segments. The equation that defines the proposed INF presented in Fig. 1 is:

$$H(f)=\begin{cases} 1, & f \le B(1-\alpha) \\ H_1(f), & B(1-\alpha) < f \le B(1-n) \\ H_2(f), & B(1-n) < f \le B(1-m) \\ H_3(f), & B(1-m) < f \le B \\ H_4(f), & B < f \le B(1+m) \\ H_5(f), & B(1+m) < f \le B(1+n) \\ H_6(f), & B(1+n) < f < B(1+\alpha) \\ 0, & f \ge B(1+\alpha) \end{cases} \tag{4}$$

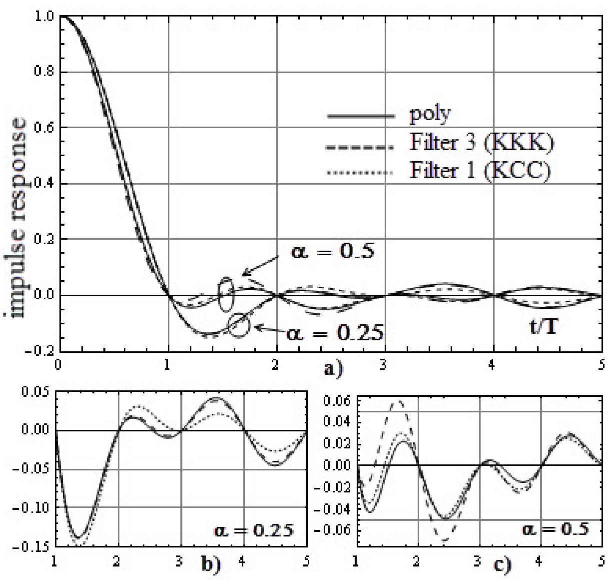

Figure 2. Impulse response of the proposed pulses generated by *KKK* and *KCC* filters, and poly pulse [8], for α = 0.25, and α = 0.5

where $B > 0$ is the bandwidth equivalent to symbol repetition rate $T = 1/(2B)$, α is the excess bandwidth, $0 \le \alpha \le 1$, *m, n, a,* and *b* (observe Fig.1) are used as coordinates of the delimiting points, respectively.

The impulse response is obtained from the inverse Fourier transforms of the $H_i(f)$ component functions.

The contributions $p_i(t)$ of the six component parabolic pieces of the frequency characteristic $H(f)$, ($i=\overline{1,6}$) to the time response $p(t)$ are:

$$p_i(t)=\int_{x_{0i}}^{x_{1i}} H_i(f)\cos(2\pi f t)\,df \tag{5}$$

For B=1, they are given by:

$$\begin{aligned} p_i(t)=&\frac{2\pi t(x_{0i}-x_{1i})(y_{0i}-y_{1i})\cos(2\pi t x_{1i})}{4\pi^3t^3(x_{0i}-x_{1i})^2}+\\ &+\frac{\left(y_{1i}-\left(1+2\pi^2t^2(x_{0i}-x_{1i})^2\right)y_{0i}\right)\sin(2\pi t x_{0i})}{4\pi^3t^3(x_{0i}-x_{1i})^2}+\\ &+\frac{\left(y_{0i}-\left(1-2\pi^2t^2(x_{0i}-x_{1i})^2\right)y_{1i}\right)\sin(2\pi t x_{1i})}{4\pi^3t^3(x_{0i}-x_{1i})^2} \end{aligned} \tag{6}$$

The coordinate values x_{0i}, x_{1i}, y_{0i}, and y_{1i} are tabulated in Table I for the filter 1 with *KKC* configuration (concave-concave-convex).

The time response is obtained as

$$p(t)=\sum_{i=0}^{6} p_i(t) \tag{7}$$

with

$$p_0(t)=\int_0^{B(1-\alpha)}\cos(2\pi f t)\,df=\frac{\sin(2B(1-\alpha)\pi t)}{2\pi t} \tag{8}$$

All filters have closed-form impulse responses.

For instance, the impulse response for the *KKK* filter denoted as $A_1A_2A_3A_4'A_5'A_6'$ was obtained as

$$h_3(t)=\frac{2\sin(\pi t)}{m^2(\alpha-n)^2(m-n)^2\pi^3t^3}\,g(t) \tag{9}$$

with:

$$\begin{aligned} g(t)=&\Big(2(1-b)m^2(m-n)^2\cos(\pi\alpha t)-\\ &2m^2\left(m^2-b(\alpha^2+m^2\right)+a(\alpha-n)^2+\\ &\left(2\left(\alpha b-(1-b)m\right)n+(1-2b)n^2\right)\cos(\pi n t)\Big)+\\ &(\alpha-n)\Big((\alpha-n)\big((4a-2b-1)m^2+\\ &2(1-2a)mn+(2a-1)n^2\big)\cos(\pi m t)+\\ &(m-n)^2\big(2(1-b)m^2\pi t\sin(\pi\alpha t)+\\ &(1-2a)(\alpha-n)(1-\pi m t\sin(\pi m t))\big)\Big)+\\ &2(a-b)m^2(\alpha-n)^2(m-n)\pi t\sin(\pi n t) \end{aligned} \tag{10}$$

In Fig. 2 are represented several side lobes of the time response of the *KKK* and *KCC* filter using as a reference the *poly* pulse [8]. Their smaller slope in the vicinity of ideal sampling moments will determine a decay of the magnitude of first order side lobes, which in turn leads to a reduced value of the error probability.

III. SIMULATIONS RESULTS AND DISCUSSIONS

In this section we provide a coverage analysis and ISI error probability results for the frequency characteristic model described earlier.

The error probability P_e was determined using Fourier series as in [11]:

$$P_e = \frac{1}{2} - \frac{2}{\pi} \sum_{\substack{m=1 \\ M\ odd}}^{M} \left(\frac{\exp\left(-m^2\omega^2/2\right)\sin\left(m\omega g_0\right)}{m} \right) \prod_{k=N_1}^{N_2} \cos\left(m\omega g_k\right) \tag{11}$$

In Eq. (11), M represents the number of coefficients considered in the approximate Fourier series of noise complementary distribution function; $\omega = 2\pi/T_f$ - angular frequency; T_f is the period used in the series; N_1 and N_2 are the number of interfering symbols before and after the transmitted symbol; $g_k = p(t-kT)$ where $p(t)$ is the impulse response used for transmission, and T is the bit duration. The results are computed using $T_f = 40$ and $M = 61$ for $N=2^9$ interfering symbols and SNR=15 dB.

In Figs. 2(b), and 2(c) are represented in detail a few lateral lobes of the time response generated by two filters of the proposed set F of 8 filters (Filter 3 - *KKK*, and Filter 1 - *KCC)*. The size of first largest side lobes decreased, which in turn determined the decrease of the the error probability.

The error probability was calculated when the parameters m and n, which interfere in filters design, span the interval $(0, \alpha)$, and the a and b take values in the interval $[0.01, 0.99]$ with a step of 0.01, assuming usual values of the timing offset (t/T) equal to *0.05*, *0.1*, and *0.2* and three usual values of excess bandwidth α (*0.25*, *0.35*, and *0.5*).

A detailed analysis was performed, studying the evolution of error probability when different values of parameters which interfere in filters design were used. We obtained minimal values of error probability, presented in Table II. It should be mentioned that the values of the error probability were obtained for the same set of values of *m, n, a*, and *b* for a particular values of the excess bandwidth α, and by consequence they are not minimal for all filters.

The performance of the new set of proposed pulses is compared with that of the *poly* pulse [8], used as a reference. Most results, marked with bold characters in Table II, with the suggested values of design parameters (*m*, *n*, *a*, and *b*), outperform those obtained for the 4^{th} degree POLY pulse [8], for the same values of excess bandwidth α, timing offset t/T, SNR, and number of interfering pulses. The values (*m*, *n*, *a*, *b*) were determined as shown above. The same approach was used in [6], [8], [10], [13], [14], [15] and [16].

From Table II, it can be inferred that for a small value of the timing offset (t/T=0.05), and the usual values of *α=0.25*, *0.35*, and *0.5*, the best results for error probability are obtained with *KKK* filter.

Improved results are obtained when using two adjacent concave pieces (e.g. Filter 4 - *CKK*, and Filter 5 - *KKC*). For higher values of timing offset (t/T=0.2), it is observed that improvements are obtained when using three or two adjacent convex pieces (e.g. Filter 2- *CCC*, and Filter 1 - *KCC*).

TABLE II. ISI ERROR PROBABILITY FOR $N = 2^9$ INTERFERING SYMBOLS AND $SNR = 15dB$

α	P_e (*m, n, a, b*)	t/T=0.05	t/T=0.1	t/T=0.2
	poly	4.734×10^{-8}	8.834×10^{-7}	2.241×10^{-4}
	acos[asinh]	5.148×10^{-8}	9.9816×10^{-7}	2.494×10^{-4}
	POWER (β=0.25)	4.576×10^{-8}	8.243×10^{-7}	2.048×10^{-4}
	(0.11, 0.24,0.62,0.78) Filter 1 (KCC)	4.873×10^{-8}	8.909×10^{-7}	**2.145×10^{-4}**
0.25	Filter 2 (CCC)	4.936×10^{-8}	9.172×10^{-7}	**2.236×10^{-4}**
	Filter 3 (KKK)	**4.646×10^{-8}**	**8.297×10^{-7}**	**2.012×10^{-4}**
	Filter 4 (CKK)	**4.708×10^{-8}**	**8.555×10^{-7}**	**2.102×10^{-4}**
	Filter 5 (KKC)	**4.679×10^{-8}**	**8.377×10^{-7}**	**2.026×10^{-4}**
	Filter 6 (CKC)	4.741×10^{-8}	**8.635×10^{-7}**	**2.117×10^{-4}**
	Filter 7 (KCK)	4.841×10^{-8}	8.845×10^{-7}	**2.140×10^{-4}**
	Filter 8 (CCK)	4.903×10^{-8}	9.109×10^{-7}	**2.232×10^{-4}**
	poly	3.290×10^{-8}	3.839×10^{-7}	6.563×10^{-5}
	acos[asinh]	3.412×10^{-8}	4.041×10^{-7}	6.765×10^{-5}
	acos[acos]	3.275×10^{-8}	3.796×10^{-7}	6.434×10^{-5}
	asech[acos]	3.226×10^{-8}	3.736×10^{-7}	6.449×10^{-5}
	asech[asech]	3.225×10^{-8}	3.727×10^{-7}	6.411×10^{-5}
	asech[exp]	3.259×10^{-8}	3.777×10^{-7}	6.444×10^{-5}
	POWER (β=0.33)	3.103×10^{-8}	3.564×10^{-7}	6.434×10^{-5}
0.35	(0.15, 0.34,0.62,0.78) Filter 1 (KCC)	**3.205×10^{-8}**	**3.590×10^{-7}**	**5.857×10^{-5}**
	Filter 2 (CCC)	**3.240×10^{-8}**	**3.667×10^{-7}**	**6.074×10^{-5}**
	Filter 3 (KKK)	**3.069×10^{-8}**	**3.492×10^{-7}**	**6.243×10^{-5}**
	Filter 4 (CKK)	**3.104×10^{-8}**	**3.586×10^{-7}**	**6.498×10^{-5}**
	Filter 5 (KKC)	**3.088×10^{-8}**	**3.506×10^{-7}**	**6.187×10^{-5}**
	Filter 6 (CKC)	**3.123×10^{-8}**	**3.598×10^{-7}**	**6.438×10^{-5}**
	Filter 7 (KCK)	**3.188×10^{-8}**	**3.597×10^{-7}**	**6.000×10^{-5}**
	Filter 8 (CCK)	**3.223×10^{-8}**	**3.686×10^{-7}**	**6.225×10^{-5}**
	poly	2.057×10^{-8}	1.354×10^{-7}	1.520×10^{-5}
	acos[asinh]	2.075×10^{-8}	1.361×10^{-7}	1.460×10^{-5}
	acos[acos]	2.005×10^{-8}	1.301×10^{-7}	1.532×10^{-5}
	asech[acos]	1.986×10^{-8}	1.295×10^{-7}	1.624×10^{-5}
	asech[asech]	1.984×10^{-8}	1.290×10^{-7}	1.605×10^{-5}
	asech[exp]	1.999×10^{-8}	1.300×10^{-7}	1.565×10^{-5}
	POWER (β=0.37)	1.945×10^{-8}	1.250×10^{-7}	1.662×10^{-5}
0.5	(0.22, 0.49,0.62,0.78) Filter 1 (KCC)	**1.945×10^{-8}**	**1.199×10^{-7}**	**1.353×10^{-5}**
	Filter 2 (CCC)	**1.961×10^{-8}**	**1.224×10^{-7}**	**1.394×10^{-5}**
	Filter 3 (KKK)	**1.919×10^{-8}**	**1.238×10^{-7}**	1.844×10^{-5}
	Filter 4 (CKK)	**1.935×10^{-8}**	**1.268×10^{-7}**	1.911×10^{-5}
	Filter 5 (KKC)	**1.922×10^{-8}**	**1.237×10^{-7}**	1.778×10^{-5}
	Filter 6 (CKC)	**1.939×10^{-8}**	**1.267×10^{-7}**	1.841×10^{-5}
	Filter 7 (KCK)	**1.946×10^{-8}**	**1.221×10^{-7}**	**1.468×10^{-5}**
	Filter 8 (CCK)	**1.962×10^{-8}**	**1.248×10^{-7}**	**1.514×10^{-5}**

IV. ANALYSIS OF SEVERAL FREQUENCY CHARACTERISTIC SCENARIOS

Driven by the need for investigation of the mechanism behind improved Nyquist filters, the objective of this section is to identify the roles of the composing parts of the filter characteristic in the frequency bands *A1*, *A2*, and *A3* delimited by $\left(B(1-\alpha), B(1-n)\right)$, $\left(B(1-n), B(1-m)\right)$, and $\left(B(1-m), B\right)$, respectively. In this section we extend the INF analysis, adding new members to the filter family investigated previously.

Fig. 3 illustrates the ISI error probability for *KKK* filter when the design parameters *m*, and *n* are those reported in Table II, and *a* and *b* take values over the entire range of definition**,** $(0.5 < a < 1$, $0.5 < b < 1)$. We studied and observed the behavior and the influence of concave shape pieces over the ISI error probability results. Varying the parameters *a*, and *b* is equivalent to changing the concavity shape of the component pieces.

First we limit our discussion at the *KKK* filter for $\alpha = 0.25$, $t/T = 0.05$, and one for $\alpha = 0.5$, $t/T = 0.2$.

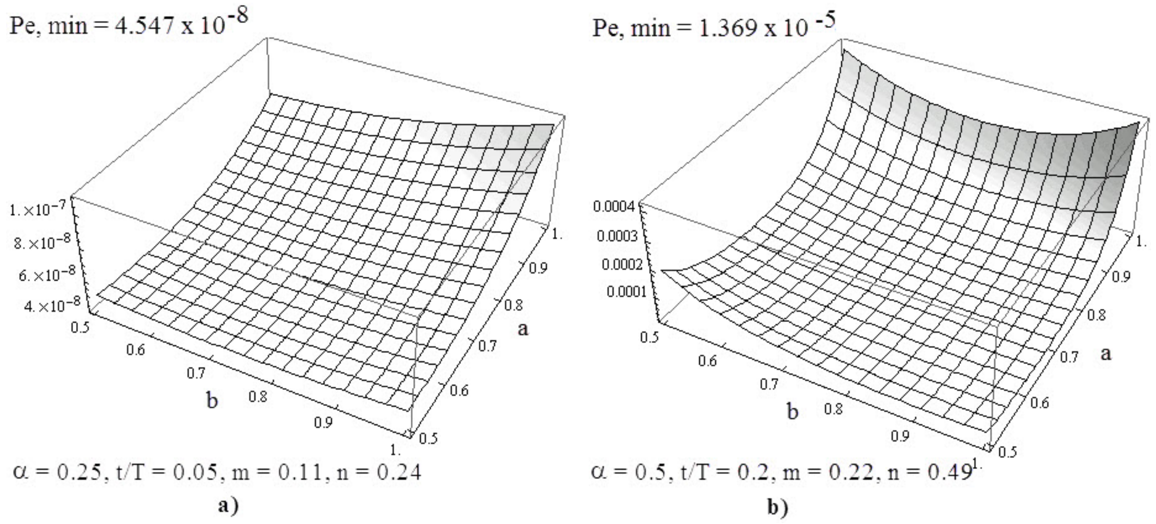

Figure 3 ISI error probability of the proposed Nyquist pulses (Filter3 - KKK) for N=2^9 interfering symbols and SNR = 15dB

Examining the values of the results presented in Fig. 3a, and Fig. 3b, we notice important enhancement for error probability. Improved results can be noticed for a large series of design parameter values *a,* and *b*.

In the first case presented in Fig. 3a, with $\alpha = 0.25$, $t/T = 0.05$, $m = 0.11$ and $n = 0.24$, the minimum value for error probability is $P_{e,\min}$=4.547×10^{-8}, which is under the value of error probability related with the *polynomial* pulse [7], P_e=4.734×10^{-8}. The same observation is valid for the second case presented in Fig. 3b, with $\alpha = 0.5$, $t/T = 0.2$, $m = 0.22$ and $n = 0.49$, where error probability is $P_{e,\min}$=1.369×10^{-5}, and is smaller than the reference results (see Table II). It can be noticed that these results are better than those presented in Table II.

As mentioned before improved results are obtained when using at least two adjacent concave pieces in the transition region beneath cut-off frequency (e.g. Filter 3 – *KKK*, Filter 4 - *CKK*, and Filter 5 - *KKC*), for a small timing offset (t/T=0.05). Next we have studied a modified filter family when one parabolic (either concave or convex) piece in the frequency characteristic is replaced with a linear one, denoted with L. It results a first new sub-family of filters with two members, (Filter 4a-*LKK*, Filter 5a–*KKL*). Afterwards we added the Filter 7a (*KLK*) to this sub-family.

The linear function $L_i(f)$ that passes through (x_1, y_1) and (x_0, y_0) is defined as

$$L_i(f) = \frac{y_1 - y_0}{x_1 - x_0}(f - x_0) + y_0 \qquad (12)$$

In Figure 4 are illustrated the transfer characteristics of the new proposed filters sub-family.

Table III contains a comparison of the values of ISI error probability for the new sub-family of filters with a linear piece in the transfer characteristic for $\alpha = 0.25, 0.35, 0.5$, and usual values of the timing offset t/T $(0.05, 0.1, 0.2)$.

We kept the same set of values as in previous section (Table II). Comparing the results from Table III and Table II we observe a decrease of error probability when using a linear piece (*L*) instead of a convex one (*C*), (Filter 4a - *LKK*, Filter 5a – *KKL*). Analyzing the results reported in Table III, we observe that Filter 5a - *KKL* has an improved behavior in terms of probability of error caused by ISI, as compared to Filter 4a – *LKK*. For $t/T = 0.2$, Filter 5a – *KKL* performs better than Filter 4 – *KKK* for all values of roll-off factor ($\alpha = 0.25, 0.35, 0.5$).

In Fig. 4 we have plotted the ISI error probability for Filter 4a - *LKK*, when the design variables *m*, and *n* are those reported in Table II, and *a* and *b* are varied over the domain ($0.5 < a < 1$, $0.5 < b < 1$). We studied and observed the behavior and the influence of linear pieces (*L*) over the ISI error probability results.

We observed in Fig. 4a and Fig. 4b that the minimum values for error probability are $P_{e,\min}$=4.574×10^{-8} ($\alpha = 0.25$, $t/T = 0.05$, $m = 0.11$ and $n = 0.24$) and $P_{e,\min}$=1.386×10^{-5} ($\alpha = 0.5$, $t/T = 0.2$, $m = 0.22$ and $n = 0.49$), which are under the error probability reported for the *poly* pulse [8].

TABLE III. ISI ERROR PROBABILITY FOR N = 2^9 INTERFERING SYMBOLS AND SNR = 15dB

α	P_e (*m, n, a, b*)	t/T=0.05	t/T=0.1	t/T=0.2
0.25	poly	4.734x10^{-8}	8.834x10^{-7}	2.241x10^{-4}
	(0.11,0.24,0.62,0.78)			
	Filter 3 (KKK)	4.646x10^{-8}	8.297x10^{-7}	2.012x10^{-4}
	Filter 4 (CKK)	4.708x10^{-8}	8.555x10^{-7}	2.102x10^{-4}
	Filter 4a (LKK)	4.6737x10^{-8}	8.408x10^{-7}	2.0500x10^{-4}
	Filter 5 (KKC)	4.679x10^{-8}	8.377x10^{-7}	2.026x10^{-4}
	Filter 5a(KKL)	4.6523x10^{-8}	8.2840x10^{-7}	1.998x10^{-4}
	Filter 7 (KCK)	4.841x10^{-8}	8.845x10^{-7}	2.140x10^{-4}
	Filter 7a (KLK)	4.7213x10^{-8}	8.4609x10^{-7}	2.0336x10^{-4}
0.35	poly	3.290x10^{-8}	3.839x10^{-7}	6.563x10^{-5}
	(0.15,0.34,0.62,0.78)			
	Filter 3 (KKK)	3.069x10^{-8}	3.492x10^{-7}	6.243x10^{-5}
	Filter 4 (CKK)	3.104x10^{-8}	3.586x10^{-7}	6.498x10^{-5}
	Filter 4a (LKK)	3.0843x10^{-8}	3.5313x10^{-7}	6.3438x10^{-5}
	Filter 5 (KKC)	3.088x10^{-8}	3.506x10^{-7}	6.187x10^{-5}
	Filter 5a(KKL)	3.069 x10^{-8}	3.4664x10^{-7}	6.110x10^{-5}
	Filter 7 (KCK)	3.188x10^{-8}	3.597x10^{-7}	6.000x10^{-5}
	Filter 7a(KLK)	3.1078x10^{-8}	3.4790x10^{-7}	5.9190x10^{-5}
0.5	poly	2.057x10^{-8}	1.354x10^{-7}	1.520x10^{-5}
	(0.22,0.49,0.62,0.78)			
	Filter 3 (KKK)	1.919x10^{-8}	1.238x10^{-7}	1.844x10^{-5}
	Filter 4 (CKK)	1.935x10^{-8}	1.268x10^{-7}	1.911x10^{-5}
	Filter 4a (LKK)	1.9255x10^{-8}	1.2500x10^{-7}	**1.8683x10^{-5}**
	Filter 5 (KKC)	1.922x10^{-8}	1.237x10^{-7}	1.778x10^{-5}
	Filter 5a(KKL)	**1.9113x10^{-8}**	1.2197x10^{-7}	1.7623x10^{-5}
	Filter 7 (KCK)	1.946x10^{-8}	1.221x10^{-7}	1.468x10^{-5}
	Filter 7a(KLK)	1.9138x10^{-8}	1.1982x10^{-7}	1.5671x10^{-5}

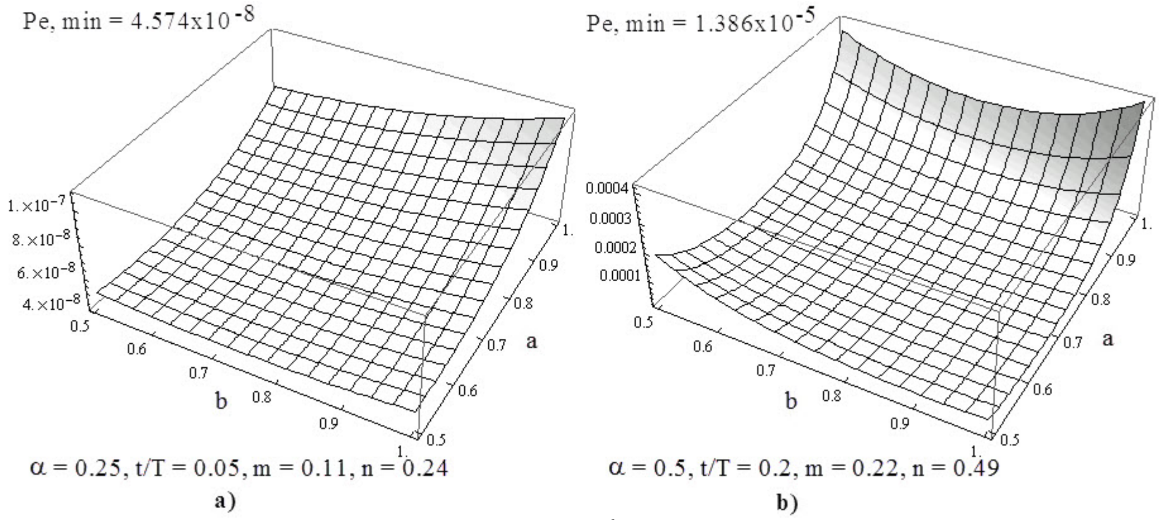

Figure 4. Error probability of the senary Nyquist pulses (Filter 4a - LKK) for N=2^9 interfering symbols and SNR = 15dB

These minimum values of the probability of error are significantly better than those reported in Table III, for the same set of values of *m, n, a*, and *b* and particular values of the excess bandwidth α.

Interesting results and significant improvements are obtained for Filter 7a – *KLK*, particularly for $t/T = 0.2$, and $\alpha = 0.25, 0.35, 0.5$.

In order to show that we have obtained fairly significant improvements, we have plotted in Fig. 6 the ISI error probability for *KLK* filter when the design variables *m*, and *n* are those reported in Table II, and *a* and *b* are varied in the range ($0.5 < a < 1$, $0.5 < b < 1$).

Fig. 5 illustrates several significant side lobes of the time response generated by *KLK* and *KKK* filters, for three values of the excess bandwidth ($\alpha = 0.25, 0.35, 0.5$). There is a decrease of the size of first side lobes that will manifest itself in the reduction of the error probability value.

In Fig. 6 we have plotted the ISI error probability for *KLK* filter when the design variables *m*, and *n* are those reported in Table II, and *a* and *b* are varied over the domain ($0.5 < a < 1$, $0.5 < b < 1$).

We studied and observed the behavior and the influence of linear pieces (*L*) on the error probability results. Varying the parameters values *a*, and *b* is equivalent to changing the slope of the linear piece (*L*), and the concavity shape of the component pieces (*K*).

An analysis of the results in Fig. 6a, and Fig. 6b, shows consistent potential for error probability improvement.

The improved behavior can be detected for a wide range of design parameter values, *a* and *b*.

A result in Fig. 6a, with $\alpha = 0.35$, $t/T = 0.05$, $m = 0.15$ and $n = 0.34$ is $P_{e,\min}$=3.0412×10^{-8}.

This is below the error probability reported for *poly* pulse [7], P_e=3.290×10^{-8}.

The same remark stands in the second case plotted in Fig. 6b, with $\alpha = 0.5$, $t/T = 0.2$, $m = 0.22$ and $m = 0.49$, where error probability is $P_{e,\min}$=1.358×10^{-5}, and is below the reference values (see Table II and Table III). These results are better than those in Table III.

Observing that the variation of parameters a and b has a quite important influence on error probability, we also investigated the filter sub-family *KKL-LKK-KLK*, when $a = b$.

Imposing $a = b$ leads to the introduction of a constant piece in the filter transfer characteristic. This results in complexity reduction of the impulse response expression.

The values of the minimum error probability are reported in Table IV.

V. Conclusion

We have introduced a new family of inter-symbol interference free pulses generated by INFs with the aim to examine in detail new methods for constructing families of Nyquist pulses.

We observed that for small values of the timing offset (t/T=0.05), the best outcomes for error probability are obtained when using three or two adjacent concave pieces in the transition region close to cut-off frequency.

For higher values of timing offset (t/T=0.2) and excess bandwidth, improved results are obtained when using three or two adjacent convex pieces in the transition region close to Nyquist frequency.

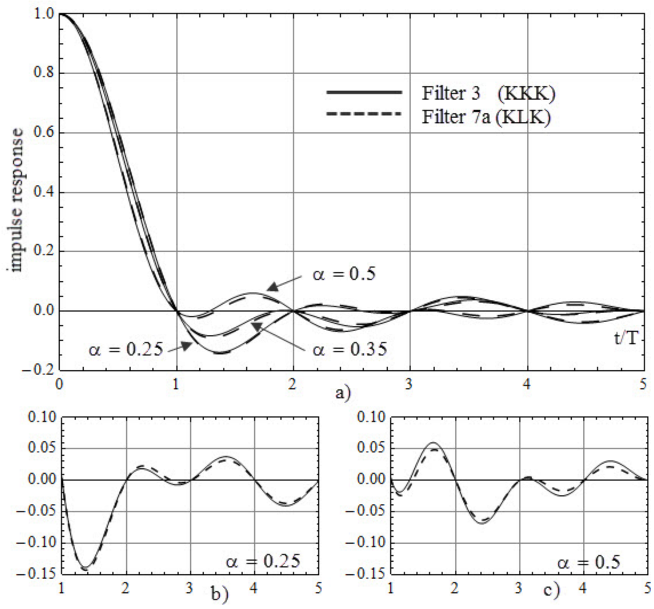

Figure 5. Time response of new proposed pulses generated by Filter 3 - KKK, and Filter 7a - KLK filters, for α = 0.25, α = 0.35, and α = 0.5

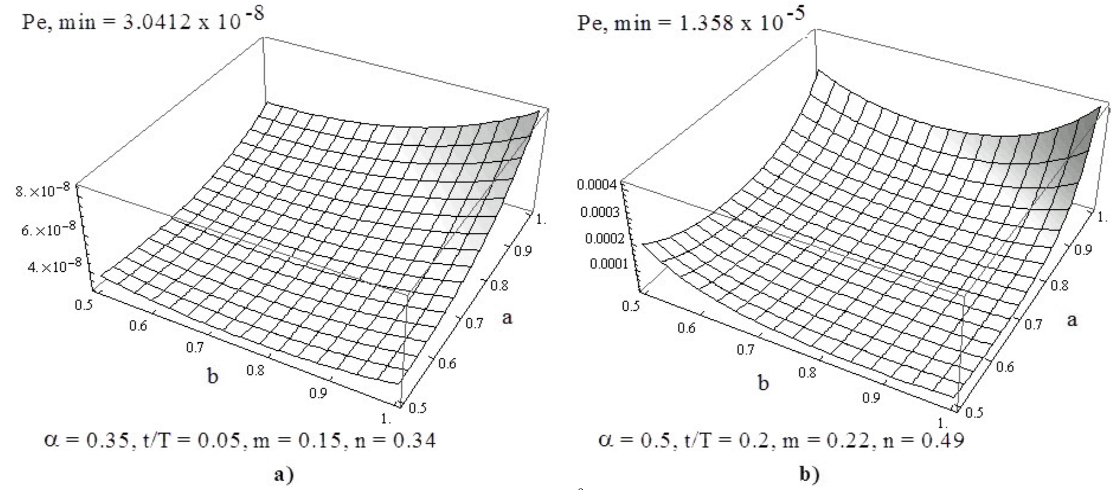

Figure 6. ISI error probability of senary Nyquist pulses (Filter 7a - KLK) for N=2^9 interfering symbols and SNR = 15dB

TABLE IV ISI ERROR PROBABILITY FOR N = 2^9 INTERFERING SYMBOLS AND SNR = 15DB

P_e (*m, n*) α		t/T=0.05	t/T=0.1	t/T=0.2
0.25	poly	4.734×10^{-8}	8.834×10^{-7}	2.241×10^{-4}
	m=0.11, n=0.24, a=0.62, b=0.78: Filter 3, Filter 4, Filter5, Filter7 m=0.11, n=0.24, a = b: Filter 4b, Filter 5b, Filter 7b			
	Filter 3 (KKK)	4.646×10^{-8}	8.297×10^{-7}	2.012×10^{-4}
	4 (CKK)	4.708×10^{-8}	8.555×10^{-7}	2.102×10^{-4}
	4b(LKK)	4.584×10^{-8} (a=b=0.62)	8.379×10^{-7} (a=b=0.65)	2.078×10^{-4} (a=b=0.67)
	5 (KKC)	4.679×10^{-8}	8.377×10^{-7}	2.026×10^{-4}
	5b(KKL)	4.566×10^{-8} (a=b=0.61)	8.343×10^{-7} (a=b=0.64)	2.073×10^{-4} (a=b=0.66)
	7 (KCK)	4.841×10^{-8}	8.845×10^{-7}	2.140×10^{-4}
	7b(KLK)	4.560×10^{-8} (a=b=0.62)	8.291×10^{-7} (a=b=0.65)	2.049×10^{-4} (a=b=0.67)
0.35	poly	3.290×10^{-8}	3.839×10^{-7}	6.563×10^{-5}
	m=0.15, n=0.34, a=0.62, b=0.78: Filter 3, Filter 4, Filter5, Filter7 m=0.15, n=0.34, a = b: Filter 4b, Filter 5b, Filter 7b			
	3 (KKK)	3.069×10^{-8}	3.492×10^{-7}	6.243×10^{-5}
	4(CKK)	3.104×10^{-8}	3.586×10^{-7}	6.498×10^{-5}
	4b(LKK)	3.082×10^{-8} (a=b=0.65)	3.628×10^{-7} (a=b=0.68)	6.534×10^{-5} (a=b=0.7)
	(KKC)	3.088×10^{-8}	3.506×10^{-7}	6.187×10^{-5}
	5b(KKL)	3.079×10^{-8} (a=b=0.64)	3.652×10^{-7} (a=b=0.66)	6.689×10^{-5} (a=b=0.69)
	7 (KCK)	3.188×10^{-8}	3.597×10^{-7}	6.000×10^{-5}
	7b(KLK)	3.069×10^{-8} (a=b=0.65)	3.601×10^{-7} (a=b=0.68)	6.478×10^{-5} (a=b=0.)
0.5	poly	2.057×10^{-8}	1.354×10^{-7}	1.520×10^{-5}
	m=0.22, n=0.49, a=0.62, b=0.78: Filter 3, Filter4, Filter5, Filter7 m=0.22, n=0.49, a = b: Filter 4b, Filter 5b, Filter 7b			
	3 (KKK)	1.919×10^{-8}	1.238×10^{-7}	1.844×10^{-5}
	4 (CKK)	1.935×10^{-8}	1.268×10^{-7}	1.911×10^{-5}
	4b(LKK)	1.957×10^{-8} (a=b=0.68)	1.304×10^{-7} (a=b=0.7)	1.712×10^{-5} (a=b=0.74)
	5 (KKC)	1.922×10^{-8}	1.237×10^{-7}	1.778×10^{-5}
	5b(KKL)	1.968×10^{8} (a=b=0.67)	1.333×10^{7} (a=b=0.69)	1.827×10^{5} (a=b=0.72)
	7 (KCK)	1.946×10^{-8}	1.221×10^{-7}	1.468×10^{-5}
	7b(KLK)	1.953×10^{-8} (a=b=0.68)	1.297×10^{-7} (a=b=0.7)	1.705×10^{-5} (a=b=0.74)

Further improved results are obtained when one concave or convex piece from the transition area below cut-off frequency is replaced with a linear one with various slopes.

It can be concluded that the proposed families of ISI-free pulses provide flexibility in designing an improved pulse for a given excess bandwidth value.

The obtained results are comparable or outperform the previously reported pulses, for different values of the excess bandwidth factor α and small timing offset.

REFERENCES

[1] L. E. Franks, "Further results on Nyquist's problem in pulse transmission," IEEE Trans. Commun. Technol., vol. 16, pp. 337–340 1968. DOI: 10.1109/TCOM.1968.1089824

[2] F. S. Hill Jr., "A unified approach to pulse design in data transmission," IEEE Trans. Commun., vol. 25, pp. 346–354, 1977. DOI: 10.1109/TCOM.1977.1093828

[3] N. C. Beaulieu, C. C. Tan, M. O. Damen, "A better than Nyquist pulse," IEEE Commun. Lett., vol. 5, pp. 367 - 368, 2001. DOI: 10.1109/4234.951379

[4] N. C. Beaulieu, M. O. Damen, "Parametric construction of Nyquist-I pulses," IEEE Trans. Commun., vol. 52, pp. 2134 - 2142, 2004. DOI: 10.1109/TCOMM.2004.838739

[5] A. Assalini, A. M. Tonello, "Improved Nyquist pulses," IEEE Commun. Lett., vol. 8, pp. 87 – 89, 2004. DOI: 10.1109/LCOMM.2004.823414

[6] P. Sandeep, S. Chandan, A. K. Chaturvedi, "ISI-Free pulses with reduced sensitivity to timing errors," IEEE Commun. Lett., vol. 9, pp. 292-294, 2005. DOI: 10.1109/LCOMM.2005.1413611

[7] S. D. Assimonis, M. Matthaiou, G. K. Karagiannidis, "Two-parameter Nyquist pulses with better performance," IEEE Commun. Lett., vol. 12, pp. 807-809, 2008. DOI: 10.1109/LCOMM.2008.081117

[8] S. Chandan, P. Sandeep, A. K. Chaturvedi, "A family of ISI-free polynomial pulses," IEEE Commun. Lett., vol. 9, pp. 496-498, 2005. DOI: 10.1109/LCOMM.2005.06027

[9] S. D. Assimonis, M. Matthaiou, G. K. Karagiannidis, J. A. Nossek, "Parametric construction of improved Nyquist filters based on inner and outer functions," 2009 IEEE International Conference on Communications, Dresden, Germany, pp. 1976-1980, June 2009. DOI: 10.1109/ICC.2009.5199301

[10] N. D. Alexandru, A. L. Onofrei Balan, "Improved Nyquist filters with piece-wise parabolic frequency characteristic," IEEE Commun. Lett., vol. 15, pp. 473-475, 2011. DOI: 10.1109/LCOMM.2011.030911.102065

[11] N. C. Beaulieu, "The evaluation of error probabilities for intersymbol and cochannel interference," IEEE Trans. Commun., vol. 31, pp.1740–1749, 1991. DOI: 10.1109/26.120161

[12] S. D. Assimonis, M. Matthaiou, G. K. Karagiannidis, J. A. Nossek, "Improved Parametric Families of ISI-free Nyquist Pulses Using Inner and Outer Functions," IET Signal Processing, vol. 5, pp. 157-163, 2011. DOI: /10.1049/iet-spr.2009.0267

[13] N. D. Alexandru, M. L. Alexandru, "A Comparison of Double Convex and Double Concave Improved Nyquist Filters," Advances in Electrical and Computer Engineering, vol. 10, pp. 63-66, 2010. DOI: 10.4316/aece.2010.01011

[14] M. Mohri, M. Hamamura, "ISI-free Power Roll-Off Pulse," IEICE Trans. Fundamentals, vol. E92-A, no.10, pp. 2495-2497, 2009. DOI: 110.1587/transfun.E92.A.2495

[15] N.D. Alexandru, A. L. Balan, ISI-free pulses produced by improved Nyquist filter with piece-wise linear characteristic," Electronics Letters, vol. 47, no. 4, pp. 256–257, 2011. DOI:10.1049/el.2010.3287

[16] A.L. Balan, N. D. Alexandru, "Improved Nyquist Filters with Piecewise Rectangular-Sine Frequency Characteristics," The 9-th International Conference on Communications - COMM 2012, Bucharest, Romania, pp. 67-70, June 2012, DOI: 10.1109/ICComm.2012.6262550